Anomalous low-temperature behavior of strongly correlated Fermi systems

J. W. Clark,[1] V. A. Khodel,[1,2] and M. V. Zverev[2]
[1]*McDonnell Center for the Space Sciences and Department of Physics, Washington University, St. Louis, Missouri 63130, USA*
[2]*Russian Research Center Kurchatov Institute, Moscow 123182, Russia*
(Received 11 October 2004; published 3 January 2005)

Thermodynamic properties of Fermi systems are investigated in the vicinity of a phase transition where the effective mass diverges and the single-particle spectrum becomes flat. It is demonstrated that at very low temperatures T, the flattening of the spectrum is reflected in non-Fermi-liquid behavior of the inverse susceptibility $\chi^{-1}(T)\sim T^{\alpha}$ and the specific heat $C(T)/T\sim T^{-\alpha}$, with the critical index $\alpha=2/3$. In the presence of an external static magnetic field H, both these quantities are found to exhibit a scaling behavior, e.g., $\chi^{-1}(T,H)=\chi^{-1}(T,0)+T^{2/3}F(H/T)$, in agreement with available experimental data.

DOI: 10.1103/PhysRevB.71.012401 PACS number(s): 71.10.Hf, 71.27.+a

Manifestations of non-Fermi-liquid (NFL) behavior observed at extremely low temperatures T in a number of strongly correlated Fermi systems,[1–10] notably ^{3}He films and heavy-fermion metals, provide valuable clues to a fundamental microscopic understanding of these systems. This anomalous behavior is commonly attributed to antiferromagnetic spin fluctuations, and numerous strategies have been advanced (e.g., Ref. 11) based on integrating out all degrees of freedom except spin fluctuations. However, the spin-fluctuation model (SFM) is unable to reproduce the results of precise measurements of the inverse spin susceptibility, which, on the "metallic" side of the critical point, is found to obey $\chi^{-1}(T)\sim T^{\alpha}$ with a critical index $\alpha<1$ (cf. Refs. 1, 10, and 12). The SFM also fails to explain[6,8,10,13] the scaling exhibited by $\chi(T,H)$ in external, even tiny, static magnetic fields H. Difficulties are likewise encountered for the thermal expansion data.[14] Moreover, the SFM falls short when confronted with other generic features revealed by experiment, most notably a divergence of the effective mass $M^*(\rho)$ at a critical density $\rho=\rho_\infty$ and the emergence of NFL features even before the critical point.[1,3–5]

We are therefore compelled to explore a different strategy, in which NFL anomalies are attributed to fermionic degrees of freedom and specifically associated with flattening of the single-particle (sp) spectrum $\xi(p)$ in the immediate vicinity of ρ_∞. Near this point, the Fermi-liquid (FL) formula $\xi_{FL}(p)=p_F(p-p_F)/M^*(\rho)$ must be supplemented by terms nonlinear in $p-p_F$, since $\xi_{FL}(p;\rho)$ vanishes identically at ρ_∞. Here we shall study consequences of the alteration of $\xi(p)$ on the "metallic" side of the phase transition. Importantly, as argued below, the ratio of the damping $\gamma(\varepsilon)$ of single-particle excitations to relevant energies ε remains relatively small in this regime. Accordingly, the Landau quasiparticle formalism still applies.

We focus our attention on the real part of the ac spin susceptibility $\chi(T,\omega\to 0)$, given by the familiar FL formula[15]

$$\chi(T,\rho)=\chi_0(T,\rho)/[1-g_0(\rho)\Pi_0(T,\rho)] \tag{1}$$

in terms of the polarization Π_0, the Landau spin-spin interaction $\chi_0=-\mu_B^2\Pi_0$ (where μ_B is the Bohr magneton), and the zeroth harmonic g_0 of χ_0. To be definite, we treat the homogeneous three-dimensional (3D) case, with

$$\Pi_0(T)=\int\frac{dn[\xi(p)]}{d\xi(p)}dv\equiv-\frac{p_F^2}{\pi^2T}\int n(\xi)[1-n(\xi)]\frac{dp}{d\xi}d\xi, \tag{2}$$

where $n[\xi(p)]=1/[1+\exp(\xi(p)/T)]^{-1}$ is the quasiparticle momentum distribution and $dv=2d^3p/(2\pi)^3$. While Eqs. (1) and (2) are formally identical to familiar textbook formulas, the function $\Pi_0(T)$ can differ profoundly from its FL realization due to complicated behavior of the group velocity $d\xi(p)/dp$ in the momentum region where $|\xi(p)|\simeq T$, which dominates the integration (2).

To proceed, we invoke the well-known expression[15]

$$\frac{\partial\xi(p)}{\partial\mathbf{p}}=\frac{\mathbf{p}}{M}+\int f(\mathbf{p},\mathbf{p}_1)\frac{\partial n[\xi(p_1)]}{\partial\mathbf{p}_1}dv_1, \tag{3}$$

connecting the spectrum $\xi(p)$ and the momentum distribution $n(\xi)$ through the Landau interaction function $f(\mathbf{p},\mathbf{p}_1)$. At $T=0$, Eq. (3) implies that the effective mass M^* is related to the first harmonic $f_1(p_F,p_F)$ of the interaction function by

$$M/M^*(\rho,T=0)=1-F_1^0(\rho)/3\equiv D(\rho), \tag{4}$$

in which $F_1^0(\rho)=f_1(p_F,p_F)N_0$ with $N_0=p_FM/\pi^2$. Thus $M^*(\rho,T=0)$ diverges at the critical density ρ_∞, where $D(\rho_\infty)=0$, while at nonzero temperatures, $M^*(\rho_\infty,T)$ already has a finite value.[16] Its T dependence is found by expanding relevant quantities on both sides of Eq. (3) in Taylor series, thereby obtaining

$$d\xi/dp\simeq p_F/M^*(\rho,T)+v_2(p-p_F)^2/Mp_F \tag{5}$$

with

$$\frac{M}{M^*(T,\rho)}=D(\rho)+\frac{M}{3p_F}\int\left[(f_1'p_F^2+2f_1p_F)(p-p_F)+\left(\frac{1}{2}f_1''p_F^2+2f_1'p_F+f_1\right)(p-p_F)^2\right]\frac{\partial n[\xi(p)]}{\partial p}\frac{dp}{\pi^2}. \tag{6}$$

Here $v_2=-p_F^3Mf_1''/6\pi^2$, $f_1'=[df_1(p,p_F)/dp]_{p=p_F}$, and f_1''

$=[d^2f_1(p,p_F)/dp^2]_{p=p_F}$. The term $v_1(\rho)(p-p_F)$, which provides the contribution $v_1(\rho)(p-p_F)^2/2$ to $\xi(p)$, has been dropped in writing Eq. (5), since $v_1(\rho_\infty)$ must vanish; otherwise the function $\xi(p,\rho_\infty)$ has the same sign below and above the Fermi surface, and the Landau state becomes unstable before ρ reaches ρ_∞.

Equation (6) can be simplified using particle-number conservation, expressed approximately as

$$\int [p_F(p-p_F)+(p-p_F)^2]\frac{\partial n[\xi(p)]}{\partial p}dp=0. \qquad (7)$$

Inserting this relation into Eq. (6), we have

$$\frac{M}{M^*(T,\rho)}=D(\rho)-v_2\int\frac{(p-p_F)^2}{p_F^2}\frac{\partial n[\xi(p)]}{\partial p}dp. \qquad (8)$$

It is convenient to introduce the new variables $\tau=2TM/p_F^2$, $x=\xi(p)/T$, and $y=(p-p_F)(v_2/3MTp_F)^{1/3}$, along with $\nu=(9v_2/4)^{1/3}$ and

$$a=\int_{-\infty}^{\infty}y^2(x)e^x(1+e^x)^{-2}dx. \qquad (9)$$

In these terms, Eq. (8) reduces to $M/M^*(T,\rho)=D(\rho)+\nu a\tau^{2/3}$, while Eq. (5) becomes

$$\frac{d\xi(p,T,\rho)}{dp}=\frac{p_F}{M}[D(\rho)+\nu\tau^{2/3}(a+y^2)], \qquad (10)$$

which is recast as a relation between x and y,

$$x=y[3\nu^{-1}D(\rho)\tau^{-2/3}+3a+y^2]. \qquad (11)$$

Having solved Eqs. (11) and (9), the polarization operator $\Pi_0\equiv-N_0P_0$ is readily evaluated to yield

$$\chi(T,\rho)=\mu_B^2N_0P_0(T,\rho)/[1+G_0(\rho)D(\rho)P_0(T,\rho)], \qquad (12)$$

where $G_0=g_0p_FM^*(T=0)/\pi^2$ and

$$P_0(T,\rho)=\int_{-\infty}^{\infty}\frac{e^x(1+e^x)^{-2}}{[a+y^2(x)]\nu\tau^{2/3}+D(\rho)}dx. \qquad (13)$$

In what follows, we address systems without ferromagnetic ordering, noting that $1+G_0>0$ is sufficient for positivity of the denominator of Eq. (12). In this case, $P_0(T,\rho)$ depends crucially on the ratio $T/|\rho-\rho_\infty|$. When T drops to 0 while holding $|\rho-\rho_\infty|$ fixed, one obtains $P_0(T,\rho)=D^{-1}(\rho)$ and hence $\chi(T=0,\rho\neq\rho_\infty)=\mu_B^2N_0/[D(\rho)(1+G_0)]\sim|\rho-\rho_\infty|^{-1}$. In the opposite case, one has $D(\rho_\infty)=0$ and calculations give $M/M^*(T,\rho_\infty)\simeq0.5\nu\tau^{2/3}$ and $P_0(T,\rho_\infty)=1.2\nu^{-1}\tau^{-2/3}$. Thus we arrive at

$$\chi(T,\rho_\infty)=\chi_0(T,\rho_\infty)=1.2\mu_B^2N_0\nu^{-1}\tau^{-2/3}, \qquad (14)$$

which implies that the critical index α specifying the low-T dependence of the inverse spin susceptibility $\chi^{-1}(T,\rho_\infty)$ is 2/3. It can be verified that the corresponding one-dimensional (1D) and two-dimensional (2D) equations are identical in form to Eqs. (11) and (9), derived here for the 3D case.

The above treatment can be extended to other thermodynamic properties, notably the specific heat

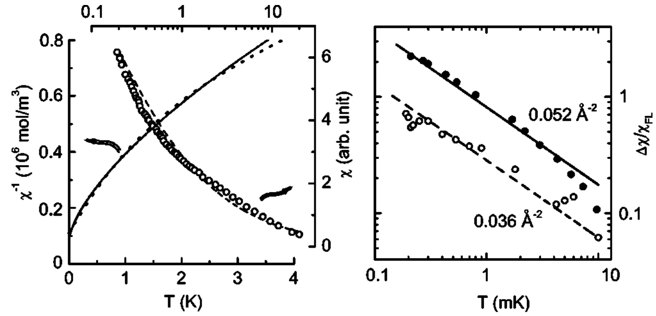

FIG. 1. Left panel, bottom-left axes: Inverse magnetic susceptibility of $YbRh(Si_{0.95}Ge_{0.05})_2$ as a function of temperature. Experimental data of Ref. 9 are shown as short dashes; the solid curve is the current prediction. Top-right axes: temperature dependence of magnetic susceptibility of $CeRu_2Si_2$ in a magnetic field of 0.02 mT. Experimental data of Ref. 8 are denoted by circles, and the theoretical prediction by the dashed curve. Right panel: Spin susceptibility excess, divided by the FL contribution to the spin susceptibility, evaluated for ^{3}He films at two densities (indicated near the curves). Experimental data from Ref. 1 appear as solid and open circles, while solid curves trace the predictions of the current theory at low T.

$$C=-\frac{p_F^2}{\pi^2}\int\xi n(\xi)[1-n(\xi)]\frac{dp}{d\xi}\frac{\partial}{\partial T}\left(\frac{\xi(T)}{T}\right)d\xi. \qquad (15)$$

Manipulations similar to those applied to $\Pi_0(T,\rho)$ yield

$$\frac{C(T,\rho)}{T}=N_0\int_{-\infty}^{\infty}\frac{x[x-2ay(x)]e^x(1+e^x)^{-2}}{[a+y^2(x)]\nu\tau^{2/3}+D(\rho)}dx, \qquad (16)$$

from which we infer that for $T\to0$ the ratio $C(T)/T$ has the same NFL behavior as the spin susceptibility.

As a rule, in electron systems of solids there exist several branches of the sp spectrum $\xi(\mathbf{p})$ that cross the Fermi surface, with the effective mass diverging in only one or two of these. (Conceivably, similar behavior occurs in 2D liquid ^{3}He.) Other branches still contribute as Landau theory dictates, providing additive T-independent terms in $\chi(T)$ and $C(T)/T$. As a result, the T-dependent excesses $\Delta\chi(T,\rho_\infty)$ and $\Delta C(T,\rho_\infty)/T$ exhibit the $T^{-2/3}$ behavior implied by Eq. (14).

To ascertain the relevance of the basic result (14) to real strongly correlated Fermi systems, we make use of available data[8–10] for the heavy-fermion metals $YbRh(Si_{0.95}Ge_{0.05})_2$ and $CeRu_2Si_2$, where the T-independent FL terms are rather small. As seen in the left panel of Fig. 1, these data are well reproduced by the proposed model. In 2D liquid ^{3}He, the FL term in $\chi(T)$ is significant. Accordingly, in this case we plot results for the excess $\Delta\chi(T)$, comparing theoretical predictions with the experimental data[1] at the two densities $\rho=0.036$ Å^{-2} and $\rho=0.052$ Å^{-2} (Fig. 1, right panel).

Let us now examine the role of damping effects. When evaluating thermodynamic properties, characteristic energies ε are of order T. We estimate the damping $\gamma(\varepsilon\sim T)$ with the help of the standard FL-theory formula,

$$\gamma(\varepsilon \sim T) \sim |\Gamma|^2[M^*(T)]^3T^2, \tag{17}$$

containing the interaction amplitude Γ and the effective mass M^*, which according to Eq. (10), depends on T as $T^{-2/3}$. It is important to recognize that the customary replacement[17] of Γ by the bare interaction V, although legitimate in ordinary Fermi liquids, is erroneous in the limit of strong correlations. The source of the error is the huge enhancement of the density of states, which suppresses Γ and makes its magnitude quite insensitive to the bare interaction.[18] To wit: summation of ladder diagrams in the particle-hole channel gives $\Gamma = V/[1+VN(0)]$, where $N(0) \sim p_F M^*$ is the density of states; hence $\Gamma \sim N^{-1}(0)$ in the limit $N(0)V \gg 1$. Inserting this result into Eq. (17), we arrive at

$$\gamma(\varepsilon \sim T)/T \sim TM^*(T)/p_F^2 \sim \tau^{1/3} \ll 1, \tag{18}$$

affirming the applicability of FL theory to our problem.

Imposition of a static external magnetic field H brings into play a new dimensionless parameter $R = \mu_B H/T$ and opens another arena for testing the model. The function $n[\xi(p)]$ entering Eq. (3) is then replaced by $[n(\xi_+(p)) + n(\xi_-(p))]/2$, where $n[\xi_\pm(p)] = [1+\exp(\xi(p)/T \pm R/2)]^{-1}$. In turn, $\xi(p)$ is determined from Eq. (5), the effective mass being the same for both spin directions at sufficiently weak H. Proceeding as before, we find

$$M/M^*(T,H,\rho_\infty) = \nu\tau^{2/3}a(R), \tag{19}$$

where

$$a(R) = \frac{1}{2}\int y^2(x)\left[\frac{e^{x+R/2}}{(1+e^{x+R/2})^2} + \frac{e^{x-R/2}}{(1+e^{x-R/2})^2}\right]dx. \tag{20}$$

In the limit $T \to 0$ or equivalently $R \to \infty$, the solution of Eq. (20) takes the analytic form $M^*(T=0,H,\rho_\infty) \sim H^{2/3}$, confirming a result of Ref. 16. Thus at sufficiently low temperatures, imposition of a static magnetic field satisfying $\mu_B H > T$ renders the effective mass $M^*(T,H,\rho_\infty)$ finite, promoting the recovery of the Landau FL theory. Along the same lines, we may establish that at the critical density ρ_∞, the magnetic moment and ac spin susceptibility display a scaling behavior, e.g.,

$$\chi_{AC}(T,H,\rho_\infty) = \mu_B^2 N_0 \nu^{-1} b(R)\tau^{-2/3}, \tag{21}$$

where

$$b(R) = \frac{1}{2}\int\left[\frac{e^{x+R/2}}{(1+e^{x+R/2})^2} + \frac{e^{x-R/2}}{(1+e^{x-R/2})^2}\right]\frac{dx}{a(R)+y^2(x)}. \tag{22}$$

Turning to the specific heat, and following the same path as taken above for $\chi(T,H)$ at the critical point, we are led to the expression

$$C(T,H,\rho_\infty)/T = N_0\nu^{-1}c(R)\tau^{-2/3}, \tag{23}$$

where

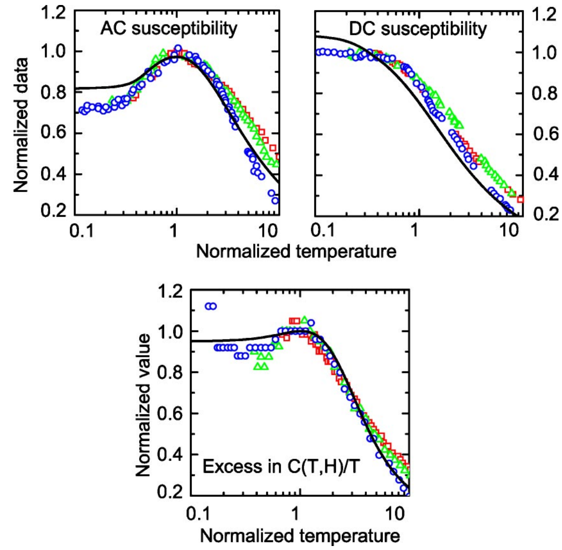

FIG. 2. (Color online) Top panels: Normalized magnetic susceptibility $\chi(T,H)/\chi(T_P)$ (top-left panel) and normalized magnetization $\mathcal{M}(T,H)/\mathcal{M}(T_P)$ (top-right panel) for $CeRu_2Si_2$ in magnetic fields 0.20 (squares), 0.39 (triangles), and 0.94 mT (circles), plotted against normalized temperature T/T_P (Ref. 8), where T_P is the temperature at peak susceptibility. The solid curves trace the universal behavior predicted by the present theory. Bottom panel: The normalized ratio $C(T,H)T_M/C(T_M)T$ for $YbRh(Si_{0.95}Ge_{0.05})_2$ in magnetic fields 0.05 (squares), 0.1 (triangles), and 0.2 T (circles) vs the normalized temperature T/T_M (Ref. 13), where T_M is the temperature at maximum ratio $C(T,H)/T$. The solid curve shows the prediction of our theory.

$$c(R) = \frac{1}{2}\int\left[\frac{[(x+R/2)^2 - 2(x+R/2)a(R)y(x)]e^{x+R/2}}{(1+e^{x+R/2})^2} + \frac{[(x-R/2)^2 - (x-R/2)a(R)y(x)]e^{x-R/2}}{(1+e^{x-R/2})^2}\right]\frac{dx}{a(R)+y^2(x)}. \tag{24}$$

A scaling behavior of this kind has been discussed by Coleman and collaborators.[6,12]

For finite H, the curve describing $\chi_{AC}(T,H)$ acquires a maximum at some temperature T_P, as does the curve for $C(T,H)/T$ at some temperature T_M. This behavior is associated with the suppression of the divergent NFL terms $\sim T^{-2/3}$ in $\chi(T,H)$ and $C(T,H)/T$ and recovery of FL behavior at static magnetic fields in which the Zeeman energy splitting $\mu_B H$ exceeds T. Following Ref. 8, Fig. 2 presents the results of numerical calculations of these quantities as functions of the normalized temperatures T/T_P and T/T_M. Demonstrably, the model developed here reproduces the experimental scaling behaviors of both the spin susceptibility[8] of the heavy-fermion metal $CeRu_2Si_2$ and the specific heat[13] of the heavy-fermion compound $YbRh(Si_{0.95}Ge_{0.05})_2$, *without any adjustable parameters*. It should be emphasized that the curves shown in Fig. 2 remain the same whether one is considering heavy-fermion metals or 2D liquid ^{3}He. This universality, a prediction of the proposed model, can be tested experimentally with the aid of an apparatus[19] designed for measurement of thermodynamic properties of 2D liquid ^{3}He in static magnetic fields.

It is seen from Eq. (2) that on the metallic side of the phase transition, the NFL behavior (14) occurs in a density interval $\Delta\rho \sim \rho_\infty \tau^{2/3}$ adjacent to the critical point. However, it will be shown in a forthcoming article that on the insulating side of the phase transition, the density range over which the NFL term $\sim T^{-2/3}$ prevails is substantially larger, $\Delta\rho \sim \rho_\infty \tau^{1/3}$.

Let us compare our results with those available within the antiferromagnetic scenario.[11] First, the proposed flattening mechanism for NFL behavior adequately explains the low-T data on the spin susceptibility, predicting $\chi^{-1}(T) \sim T^\alpha$ in the critical density region with a critical exponent $\alpha \simeq 2/3$. The spin-fluctuation model fails to provide $\alpha < 1$. Second, the flattening mechanism explains the scaling behavior $\chi^{-1} \sim T^\alpha F(H/T)$ of the spin susceptibility in static magnetic fields, whereas such a scaling property does not arise in the SFM. Third, within the model advanced here, FL behavior can be recovered at low T close to the critical point by imposing a tiny magnetic field satisfying $\mu_B H > T$. In the SFM there is no such provision for reinstating Fermi-liquid theory.

Finally, we discuss the relevance of ferromagnetic fluctuations to the NFL behavior, asserted in Refs. 8 and 10. Experimental data for most heavy-fermion systems show no evidence of ferromagnetism. The same is true for 2D liquid ^{3}He.[1,3] This implies that close to the critical point, the corresponding Pomeranchuck stability condition[15] $1+G_0(\rho) > 0$ is not violated, in spite of the divergence of the effective mass at $\rho = \rho_\infty$ and the attendant vanishing of $g(\rho_\infty)$. The value of G_0 can be estimated from the Landau sum rule[15] $\Sigma_L\{F_L/[1+F_L/(2L+1)]+G_L/[1+G_L/(2L+1)]\}=0$ by assuming all the harmonics F_L are finite except $F_1 = F_1^0 M^*/M \simeq 3M^*/M$. The Landau sum rule is then satisfied provided $G_0 \simeq -0.75$. This value of G_0 gives rise to a marked enhancement of the Sommerfeld ratio in the case $\mu_B H > T$, boosting it to a value ~ 12 that changes little when the zeroth harmonic F_0 is taken into account. Even so, such an enhancement does not in itself ensure the relevance of ferromagnetic fluctuations to the NFL behavior. Indeed, dense 3D liquid ^{3}He, with $G_0 \simeq -0.8$, exhibits no deviations from FL-theory predictions as $T \to 0$.

In summary, we have studied the impact of flattening of the single-particle spectrum on the spin susceptibility $\chi(T)$ and the specific heat $C(T)$ of strongly correlated Fermi systems. When the density approaches the critical value at which the effective mass becomes infinite, Fermi-liquid theory progressively fails as the deviant components in $\chi(T)$ and $C(T)$ grow to dominance. We have explicated the corresponding critical behavior of these components and derived a universal relation between them. Finally, our analysis has revealed the scaling behavior of $\chi(T,H)$ and $C(T,H)/T$ in the presence of an external magnetic field H. Numerical results based on this theoretical picture are in agreement with experimental data on 2D liquid ^{3}He and several heavy-fermion metals.

We thank L. P. Gor'kov, G. Kotliar, E. Krotscheck, V. R. Shaginyan, and V. M. Yakovenko for valuable discussions. This research was supported by NSF Grant No. PHY-0140316, by the McDonnell Center for the Space Sciences, and by Grant No. NS-1885.2003.2 from the Russian Ministry of Education and Science.

[1] C. Bäuerle, Yu. V. Bunkov, A. S. Chen, S. N. Fisher, and H. Godfrin, J. Low Temp. Phys. **110**, 333 (1998).
[2] C. Bäuerle, J. Bossy, Yu. M. Bunkov, A. S. Chen, and H. Godfrin, J. Low Temp. Phys. **110**, 345 (1998).
[3] A. Casey, H. Patel, J. Nyeki, B. P. Cowan, and J. Saunders, Phys. Rev. Lett. **90**, 115301 (2003).
[4] S. V. Kravchenko and M. P. Sarachik, Rep. Prog. Phys. **67**, 1 (2004).
[5] O. Prus, Y. Yaish, M. Reznikov, U. Sivan, and V. M. Pudalov, Phys. Rev. B **67**, 205407 (2003).
[6] A. Schröder, G. Aeppli, R. Caldea, M. Adams, O. Stockert, H. v. Löhneysen, E. Bucher, R. Ramazashvili, and P. Coleman, Nature (London) **407**, 351 (2000).
[7] G. R. Stewart, Rev. Mod. Phys. **73**, 797 (2001).
[8] D. Takahashi, S. Abe, H. Mizuno, D. A. Tayurskii, K. Matsumoto, H. Suzuki, and Y. Onuki, Phys. Rev. B **67**, 180407(R) (2003).
[9] R. Küchler, N. Oechler, P. Gegenwart, T. Cichorek, K. Neumaier, O. Tegas, C. Geibel, J. A. Mydosh, F. Steglich, L. Zhu, and Q. Si, Phys. Rev. Lett. **91**, 066405 (2003).
[10] P. Gegenwart, J. Custers, T. Tayama, K. Tenya, C. Geibel, O. Trovarelli, F. Steglish, and K. Neumaier, Acta Phys. Pol. B **34**, 323 (2003).
[11] A. J. Millis, Phys. Rev. B **48**, 7183 (1993).
[12] P. Coleman and C. Pepin, Physica B **312-313**, 383 (2002).
[13] J. Custers, P. Gegenwart, H. Wilhelm, K. Neumaier, Y. Tokiwa, O. Trovarelli, C. Geibel, F. Steglich, C. Pepin, and P. Coleman, Nature (London) **424**, 524 (2003).
[14] R. Küchler, P. Gegenwart, K. Heuser, E.-W. Scheidt, G. R. Stewart, and F. Steglich, Phys. Rev. Lett. **93**, 096402 (2004).
[15] L. D. Landau and E. M. Lifshitz, *Statistical Physics*, Vol. 2 (Pergamon, Oxford, 1980).
[16] V. R. Shaginyan, JETP Lett. **77**, 99 (2003); **79**, 344 (2004).
[17] P. Nozières, J. Phys. I **2**, 443 (1992).
[18] V. A. Khodel and P. Schuck, Z. Phys. B: Condens. Matter **104**, 505 (1997).
[19] C. Matsumoto, S. Murakawa, K. Honkura, C. Bäuerle, H. Kambara, and H. Fukuyama, Physica B **329-333**, 146 (2003).